Hydrodynamic Modeling of Port Foster, Deception Island, Antarctica.

Daniel Martins Figueiredo

Instituto Superior Técnico, Universidade de Lisboa, Av. Rovisco Pais, 1049-001 Lisboa, Portugal

daniel.m.figueiredo@tecnico.ulisboa.pt

Abstract: In recent years the Antarctic continent has been the place of many different studies and findings, not only for its potential but also for its conservation. Ongoing studies by Portuguese colleagues concluded that mercury concentration is rising in Deception Island, Antarctic Peninsula. One of the main problems they faced was not knowing how it would disperse inside the island, therefore giving rise to this research. Using a numerical hydrological model named MOHID, a validated tidal model was achieved and an approach to the three-dimensional model was started. Water level variations, tidal circulation and residence time were obtained. The study of the effect of stratification in the water column for both seasons (winter and summer) was performed. The recognition of internal tides generation in summer and winter was achieved and the tidal components related to it were obtained. Using lagrangean tracers, the particles circulation was depicted and the main areas of accumulation were found. It is recognized that the results of the 3D model are associated with a non-negligible uncertainty that can only be reduced with an ongoing commitment to monitoring. In this study, out of many findings, it is proved that Port Foster (Deception Island's bay) is a good place for mercury accumulation, therefore being a rising threat to the local ecosystem since it only tends to increase.

Keywords: Antarctica; Deception Island; Hydrodynamic Modeling; internal waves; mercury.

Introduction

Deception Island is located in the most remote continent on Earth in a region with severe weather conditions. The Island also presents many challenging features due to the semi-enclosed nature of the basin, the presence of hydrothermal activity and the sudden variations in topography. Little is known about mercury biogeochemistry in Antarctica, and an integrated study is needed, that takes into account the sources, fluxes, pathways and bioavailability of mercury in Port Foster ecosystem. This work, made possible through a mathematical model named MOHID, contributes to that study and also to a better understanding of the bay hydrodynamics.

Overview

Deception Island (lat. 62º57'S., long. 60º38'W) belongs to the archipelago of South Shetland Islands. It is located in

Bransfield Strait (Galindo-Zaldívar et al. 1996; Gonzalez-Casado et al. 2000), which separates the cluster of Islands from Antarctic Peninsula (Baraldo et al. 2000) (Figure 1).

Figure 1 - Location of Deception Island (Adapted from Pérez-López et al. 2007).

The Island, with a horseshoe-shaped morphology, is an active volcano, with approximately 12 km diameter and maximum altitude in Pond Mount (539 m) (Molina et al. 2013). It has an inner bay, called Port Foster, resulting from the collapse of a volcanic chimney, which allows access by the sea (Hawkes et al. 1961). Port Foster has an almost elliptical shape, with an approximate perimeter of 32 km and maximum mid-bay depth around 160 m (Pérez-López et al. 2007), being that the length and width are 9.8 e 5.7 km, respectively (Smith et al., 2003). The narrow connection existing between the bay and the sea is known as Neptune's Bellows, located southeast of the island, which presents minimum depths of 10 meters.

The tide is responsible for the variability of diurnal and semidiurnal currents. The most important tidal components are the M2, K1, O1 and S2, with the M2 being more relevant, with amplitude of 0.4 m, and the other components with amplitudes in the order of 0.28 m (Lopez et al. 1999).

The amplitudes of the velocities are very low (less than 5cm/s) within Port Foster, and the maximum tidal currents are observed in Neptune's Bellows, with speeds between 0.64 and 0.76 ms^{-1} and elevations around 3 meters during the period of spring tides (Lenn et al. 2003), being also the region where most of the tidal energy is dissipated (Vidal et al. 2011). Orographic constraints have a major influence in the winds and therefore in the wind data reliability, since in Bellingshausen Station (located in King George Island, South Shetland Islands) the predominant winds are from W and NW, the predominant winds detected by the Terrestrial Station (located in Deception Island) are from NE and SW and Comin et al. 2012 also presents one month results based in a Local WRF indicating predominant winds from NW and SE.

Tides and related processes can strongly influence the hydrography, mean circulation, and water mass exchanges in ice-covered seas (Foster et al., 1987; Padman et al., 1992; Padman, 1995). According to Lenn et al (2003), baroclinic tides are generated in Neptune's Bellows, and the study of these tides is an important issue in understanding water column mixing processes inside Port Foster. Baroclinic tides are internal waves in stratified fluids that result from the interaction of barotropic tides (generated by astronomical forcing) with topography (Levine et al. 1997).

The model used during this work was MOHID water 3D (Braunschweig et al. 2002), which since its creation has been applied to various locations, different conditions and for different purposes (Vaz

et al. 2005; Trancoso et al. 2005; Coelho et al. 1998).

Methodology

The Model Setup

The numerical computation has been carried out on a spatial domain that represent Port Foster and the surroundings through a grid consisting of 80000 rectangular elements with a horizontal resolution of $\Delta x = \Delta y = 50$ m. The parameters related with the hydrodynamics of the model are the bottom drag coefficient and the horizontal and vertical viscosities. The value assumed for bottom drag coefficient was $3x10^{-3}$, and for horizontal viscosity 3 m^2s^{-1} (This values were chosen taken into account the previous study by Vidal et al. (2010)). The vertical viscosity was obtained using General Ocean Turbulence Model (GOTM).

Bathymetry

The Bathymetry of the bay and the coastline already existed and were created by the spatial data infrastructure of the Deception island (SIMAC-IDEDEC), maintained by the Laboratory of Astronomy, Geodesy and Cartography of the University of Cadiz, Spain. It was provided to me by (Torrecillas et al, 2006). The outline bathymetry was based on a grid from the Autochart Bathymetric Map Production from NOOA. The information was processed using the software Arcgis and subsequently georeferenciated. The resulting bathymetry (Figure 2) was compared with the one presented in Barclay et al (2009) and the depths were similar for each zone.

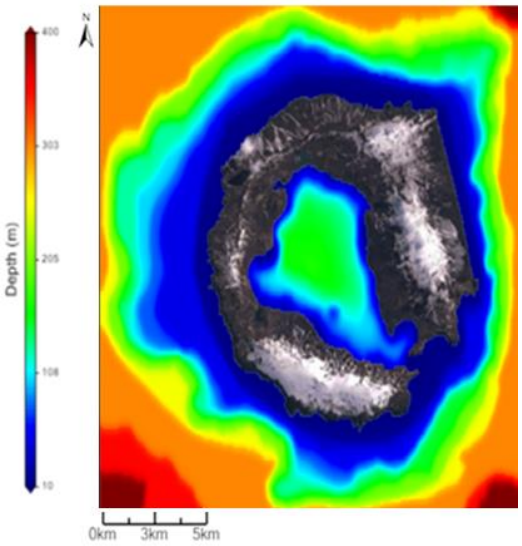

Figure 2 – Bathymetry used to run MOHID water model.

2D Model

In the 2D tidal model the tide level and the phase of the components were forced in the boundary of the domain using FES2004, which is the tide level and harmonic predictor for tide of POC-LEGOS, inputting 14 harmonic components to the model (M2, S2, K1, K2, N2, 2N2, O1, Q1, P1, M4, Mf, Mm, Mtm and MSqm).

3D Model

The 3D Model is a continuation from the validated 2D tidal model, where T-S profiles where applied with the intuition to understand their role in the currents behavior. Since there was no reliable data for winds and radiation, the profiles were frozen in time, i.e, the third term on the right-hand side of equation (1) doesn't change with time.

$$\frac{1}{\rho_0}\frac{\partial p}{\partial x_i} = \frac{1}{\rho_0}\frac{\partial p_{atm}}{\partial x_i} + g\frac{\partial \eta}{\partial x_i} + \frac{g}{\rho_0}\int_z^\eta \frac{\partial \rho'}{\partial x_i} dz \quad (1)$$

This equation gives the pressure term in the horizontal momentum equations.

Time Series Location

The locations for the time series used during this study were chosen taking into account the previous tidal data collected, the great interest to study Neptune's Bellows and also the more relevant places inside Port Foster. Figure 3 shows the time series locations with the respective identification (Table 1). For the study of mercury circulation, the sites chosen to monitor were the ones where Mão de Ferro (2012) collected the more significant mercury samples and are marked with an asterisk on the Table presented below.

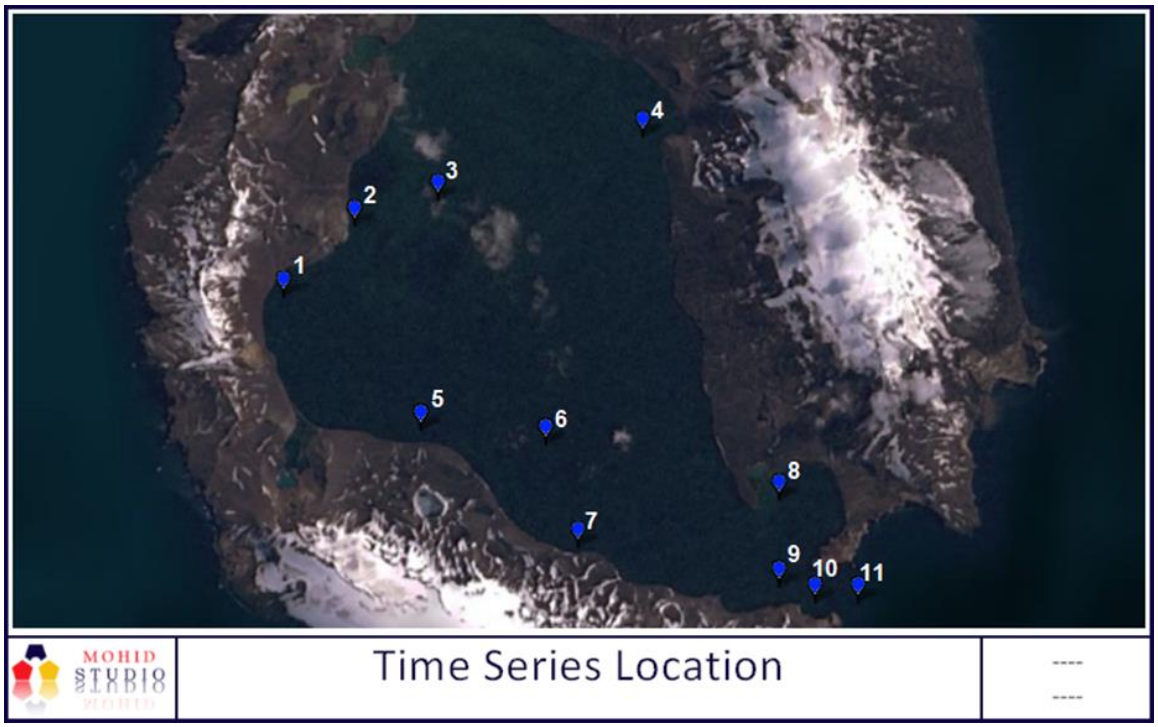

Figure 3 – Time Series Location.

Table 1 – Time Series Coordinates.

ID	Location	Latitude	Longitude
1	Near Fumaroles*	-62.9579	-60.7075
2	NW Coast*	-62.9489	-60.6877
3	Center Depth	-62.9456	-60.6645
4	Pendulum Cove	-62.9376	-60.6075
5	Between ColaFum*	-62.9748	-60.6693
6	Stanley Patch	-62.9766	-60.6345
7	Colatina*	-62.9896	-60.6255
8	Whaller's Bay	-62.9836	-60.5695
9	Inside Bellow's	-62.9946	-60.5695
10	Neptune's Bellows	-62.9966	-60.5595
11	Outside Bellows	-62.9966	-60.5475

Temperature and Salinity

The salinity and temperature profiles applied in the model were obtained by a research group during the ERUPT expeditions, where K. L. Smith et al (2003) was the chief scientist. The profiles used were collected during ERUPT III and V, which occurred in the summer and winter of 2000, respectively. The profiles chosen are representative of the inside (center image for both seasons) and outside of the island (left image for summer and right image for winter) (Figure 4).

Figure 4 – Location of the T-S profiles applied in the model (Left Image: 63º01.7'S, 60º32.0'W; Center Image: 62 º 56.7'S, 60 º 39.5'W; Right Image: 63 º 11'S, 60 º 32.606'W).

Winds and Radiation

For both winds and radiation the data available for Deception Island was scarce. For radiation, the most reliable data was from monthly average insolation that already took into account the albedo (https://eosweb.larc.nasa.gov), although hourly data is necessary for the model. For winds, raw data that was collected from March of 2004, 2006, 2007, 2009, and analyzed with the aim of understanding the predominant directions of the winds and the average wind speed. This wind data (wind speed in meters per second) was collected by R/V Laurence M. Gould Cruise during different expeditions. Since the ship was not anchored from more than a few hours in the same place, a study of wind speed and direction was done for different eight zones of Port Foster (Figure 5).

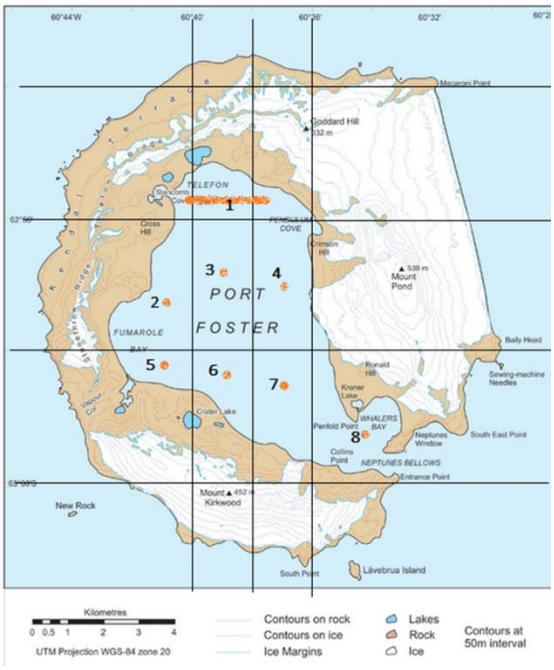

Figure 5 - Topographic map of Deception Island with the eight zones represented.

The wind speed data collected was divided between the coordinates of those zones, and for each, an event count and an average wind speed calculation were done to create wind roses.

Results

The 2D tidal model has been validated comparing the model results with "measured" sea levels. The data used is presented in Vidal et al (2010) has a result of an harmonic analysis of the tide gauge data within the island. For each constituent of each simulation, the error in the amplitudes (e_A) (Table 2) and the error in the phases (e_P) (Table 3) were calculated using equations (2) and (3).

$$e_A = \sqrt{\frac{1}{N}\sum_i \frac{(Ao_i - Am_i)^2}{2}} \qquad (2)$$

$$e_P = \frac{1}{N}\sum_i \frac{A^2_{m_i}(\theta o_i - \theta m_i)}{\sum_i A^2_{m_i}} \qquad (3)$$

The error in the amplitudes was calculated from the difference between the observations (*Ao*) and the results (*Am*) of the model, and the error in the phases was calculated from their difference ($\theta o_i - \theta m_i$), but weighted with the values of the modeled amplitudes (*Am*). N is the number of components taken into account.

Table 2 – Harmonic Analysis Results: Amplitude.

		Stations (amplitude in meters)		
		Whaller's Bay	Pendulum Cove	Colatina
M2	M	**0.3723**	**0.3729**	**0.3728**
	O	0.4600	0.4400	0.4000
S2	M	**0.2061**	**0.2065**	**0.2064**
	O	0.2800	0.2900	0.2600
O1	M	**0.2738**	**0.2738**	**0.2738**
	O	0.2900	0.2900	0.2700
K1	M	**0.3113**	**0.3115**	**0.3114**
	O	0.2600	0.2600	0.3000
e_A		**0.04**	**0.04**	**0.02**

Table 3 – Harmonic Analysis Results: Phase.

		Stations (phase in degrees relative to local time)		
		Whaller's Bay	Pendulum Cove	Colatina
M2	M	**281**	**281**	**281**
	O	280	281	283
S2	M	**360**	**360**	**360**
	O	Not Obs.	Not Obs.	351
O1	M	**49**	**49**	**49**
	O	48	55	53
K1	M	**68**	**68**	**68**
	O	66	73	74
e_P		**0.5**	**0.8**	**1.5**

The tide in Port Foster was adequately reproduced therefore the tidal model can be used with high confidence.

Model results show that the amplitudes of the velocities in Neptune's Bellows (Figure 6) can reach maximum speeds near 0.60m/s during spring tides. Currents obtained with the model are very small (less than 5 cm/s) within Port Foster. The water level variation in Neptune's Bellow (Figure 7) is depicted for 1 month simulation (from 01/07/2011 to 01/08/2011).

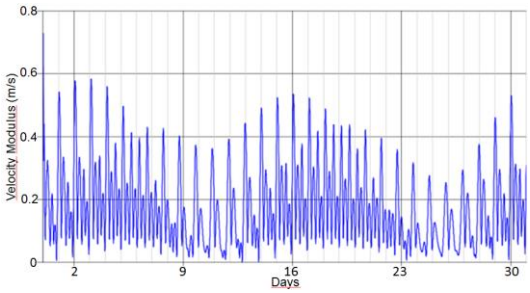

Figure 6 – Velocity Modulus in m/s.

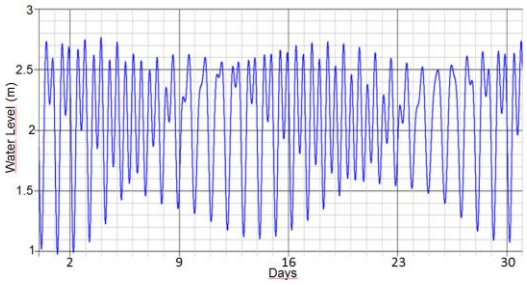

Figure 7 – Water Level Variation in m.

The velocities near the narrow channel of Neptune's Bellows show that the east-west

direction is the more important, in agreement with the orientation of the passage. The results also show that the tidal circulation has a clockwise movement during the flood tide and a counter-clockwise movement during ebb tide (Figure 8).

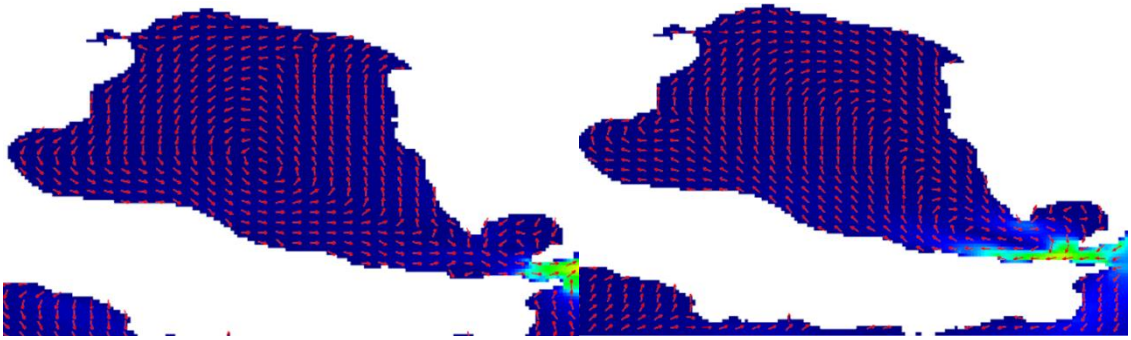

Figure 8 – Left Image: Ebb tide/Counter-clockwise; Right Image: Flood tide/Clockwise.

Residence Time

An important result is the residence time, because it gives the average amount of time a particle spends in the caldera and, therefore, its impacts. Using the following approach, the residence time was determined:

$$Tresidence = \frac{V}{Cs * Mf} \sim 1.7\ years$$

Where Volume of Port Foster (V) = 3626 hm^3; Mean Flow entering Port Foster (Mf) = 1.2 cm/s; Cross-section at Neptune's Bellows (Cs) = 5500 m^2.

This result it's close to what was expected, since Lenn et al. (2003) obtained for the residence time 2.4 years, based in a mean flow entering Port Foster of 1 cm/s. A residence time of 1.7 years is too large and explains the negative environmental impact resulting from the accumulation of metals, such as Hg.

3D Model Hydrodynamics

The velocities in both seasons vary similarly. In summer the stratification plays a major role, since the velocity Inside Bellows is sometimes higher then Neptune's Bellows velocities. Comparing the difference in amplitudes of the velocities between Neptune's Bellows (purple lines) and Inside bellows (green lines), one can see that in summer (Figure 9) this difference is smaller than in winter (Figure 10), concluding that in winter the velocities near the surface are affected by the water column mixture, slowing the tidal currents as they enter the bay.

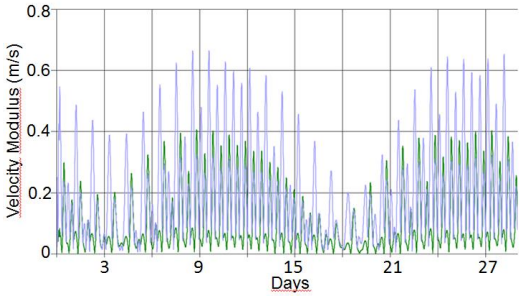

Figure 9 – Velocity Modulus: Summer.

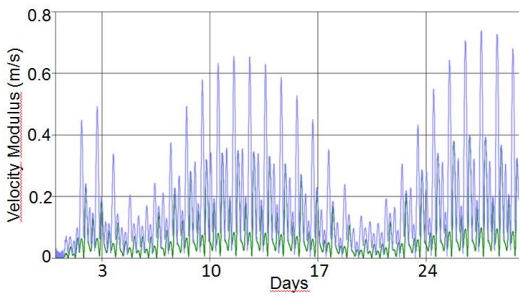

Figure 10 – Velocity Modulus: Winter.

The velocities near the bottom in all locations, except Neptune's Bellows, are close to zero meters per second. Other results also show that the velocities nearly didn't change in the center of Port Foster when comparing the 2D simulation with the 3D simulation. Although the direction Inside Bellows is slightly different in both seasons when compared with the 2D model one can conclude that stratification has more impact in summer than in winter, since in summer (Figure 11) there's an increase in the velocity magnitude near the surface.

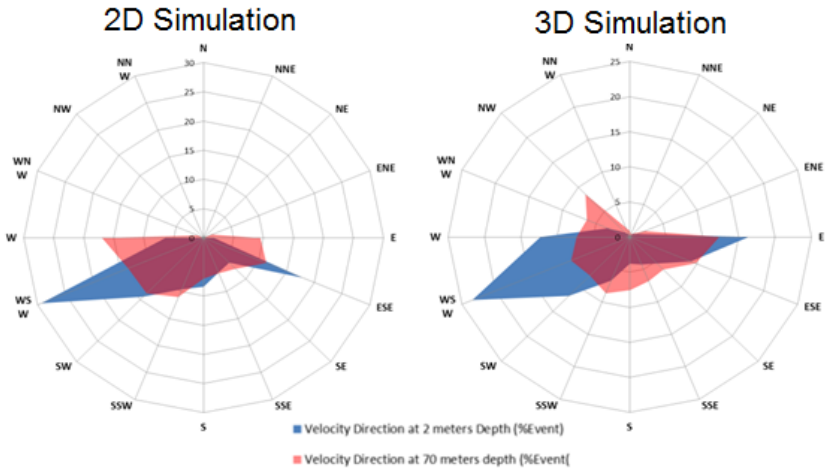

Figure 11 – Inside Bellows: Velocity Direction and Magnitude for summer.

In another analysis, the Buoyancy frequency was depicted for summer and winter inside Port Foster. The frequency quantifies the importance of stability, and it is a fundamental variable in the dynamics of a stratified flow. The thermocline (locations with a sharp change in temperature) in summer is located between 10 and 20 meters (Figure 12), while in winter is not really present, since the water column is well mixed (Figure 13).

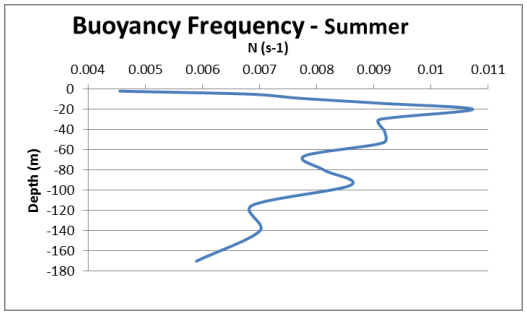

Figure 12 – Buoyancy Frequency: Summer.

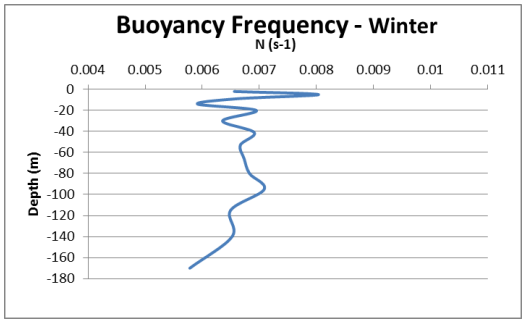

Figure 13 – Buoyancy Frequency: Winter.

Particles, such as mercury, are expected to stay above the thermocline in the summer because of the stratification. In winter, since the water column is well mixed they're expected to be dispersed in the water column.

Internal Tides

In the study of internal tides it was important to know if they could be formed during Summer and Winter, and which components were most likely associated to

its origin. The tidal components that can be associated with internal tides generation in Neptune's Bellows are the ones above the black line plotted in Figure 14 (since the frequency band for internal waves propagation is between the Coriolis and Buoyancy frequency).

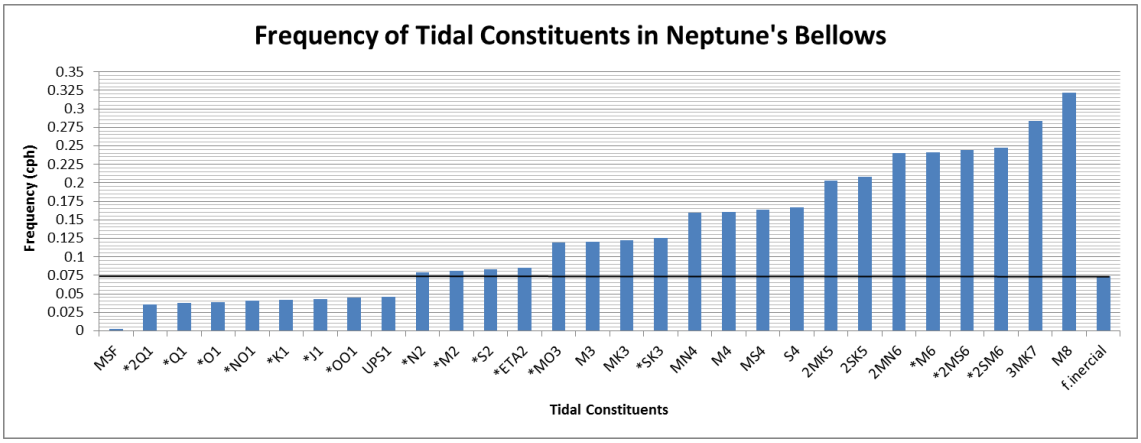

Figure 14 – Frequency of tidal constituents in Neptune's Bellows.

An indication of the potential generation sites of internal tides, has well has the more important components related to their appearance, can be deduced from the linear internal wave theory, whereby the bottom slope (bs) is compared with the slope of the internal wave characteristics (c), as defined by (Baines 1982; Craig 1987):

$$c^2 = \frac{w^2 - f^2}{N^2 - w^2} \qquad (4)$$

Where f, N, and w are the inertial, Buoyancy, and tidal frequencies, respectively. Regions where the ratio α between bs and c is equal or higher than 1 are likely sites for internal tide generation. Where the ratio α is less than 1, it is not to be expected that internal tides should be generated. If α = 1, the internal tide generated will propagate along slope and if α > 1, it will propagate in an offshore direction (Pereira & Castro 2007).

The following graphs depict the results using the approach mentioned above. The location is Neptune's Bellows, for both summer (Figure 15) and winter (Figure 16) situations. The component presented is M2.

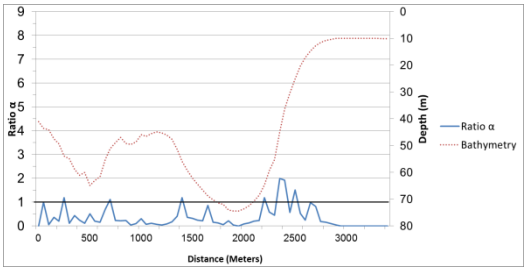

Figure 15 – Summer: Ratio alpha as function of Depth and Distance.

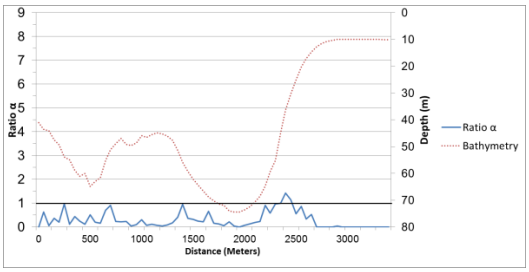

Figure 16 – Winter: Ratio alpha as function of Depth and Distance.

From figures 15 and 16, one can conclude that internal tides can be generated in summer and also in winter, due to temperature and salinity stratification, respectively. In this study an analysis to N2 and SK3 can be also seen, where it is concluded that N2 and M2 are associated

with internal tides generation, but SK3 can be discarded since it has no influence.

Wind Results

The results presented in the full study are more in agreement with the predominant winds detected at the Terrestrial Station (NE and SW), then those observed at Bellingshausen Station where the predominant direction is from W and NW.

Mercury Circulation

One of the main objectives of this work was too see how the tide influences the particles circulation within the bay and whether the stratification plays a important role in their dispersion. After one month simulation, the conclusions are that there is a poor rate exchange of water between Port Foster and the surroundings, the particles tend to accumulate in the west to north part of the bay due to the fact that the velocities gradually decrease from Neptune's Bellows to that region (Figure 17).

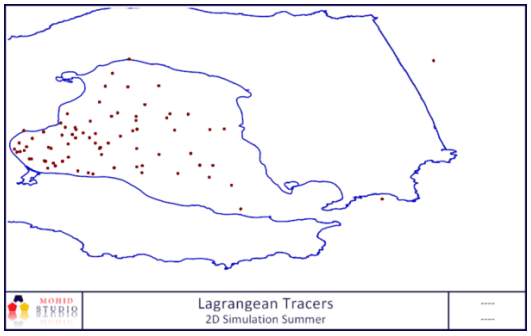

Figure 17 – summer: Lagrangean Tracers 2D Simulation.

Conclusions

The tidal model was validated with success. The hydrodynamic 2D Model also confirms known findings. The general circulation inside Port Foster is presented, showing the variation in water level, the ebb/flood tides and the residence time. A 3D simulation was performed. To the best of our knowledge, such an analysis was never done before. The 3D model presented in this work only takes into account the fluid stratification, since the temperature and salinity profiles were considered steady. Due to the absence of data, the model couldn't be validated, limiting its ability to make predictions and allowing only to study processes. The stratification plays a bigger role in the summer. The tidal currents direction is not affected by the changes in density but the magnitude of velocities are. There's a strong evidence of the generation of internal waves in Neptune's Bellows in both seasons. The impact of the energy released in this process in Port Foster's water column is yet to be assessed. The M2 and N2 are the two main tidal components related to this phenomenon. One of the most important findings is that Port Foster presents a large residence time, of almost 1.7 years. This finding, plus past studies with almost the same value, proves that the bay is a good place for mercury accumulation, therefore being a rising threat to the local ecosystem. Lagrangean tracers confirmed this conclusion.

References

Baines, P. G. (1982). On internal tide generation models. Deep-Sea Res. A, 29, 307–338.

Baraldo, A., Rinaldi, C.A. (2000), Stratigraphy and structure of Deception Island, South Shetland Islands, Antarctica, Journal of South American Earth Sciences 13(2000) 785-796.

Braunschweig, F., Leitao, P. C., Fernandes, L., Pina, P., Neves. (2002). The object oriented design of the integrated Water Modelling System, 1–12.

Barclay, a. H., Wilcock, W. S. D. & Ibáñez, J. M. (2009). Bathymetric constraints on the tectonic and volcanic evolution of Deception Island Volcano, South Shetland Islands. Antarctic Science, 21(02), p.154-163.

Coelho, H. S., Neves, R. R., Leitão, P. C., Martins, H. & Santos, A. P. (1999). The slope current along the western European margin: A numerical investigation. Boletin Instituto Espanol de Oceanografia. 15, 1998, pp. 61-72.

Comin, A. N., Acevedo, O. C., Souza, R. B. (2012). Comparison Between in situ Thermodynamic Parameters and the WRF Model in high resolution out in Deception Island, Antarctica. Climate change, Impacts and Vulnerabilities in Brazil: Preparing the Brazilian Northeast for the future.

Craig, P. D. (1987). Solutions for the internal tide generation over coastal topography. J. Mar. Res., 45, 83–105.

Galindo-Zaldívar J., A. Jabaloy, A. Maldonado and C. Sanz de Galdeano (1996), Continental fragmentation along the South Scotia Ridge transcurrent plate boundary (NE Antarctic Peninsula), Tectonophysics, 259, 275-301.

González-Casado, J.M., J.L. Giner-Robles & J. López-Martínez (2000), Bransfield Basin, Antarctic Peninsula: not a normal backarc basin, Geology, 28, 1043-1046.

Hawkes, D. D. (1961). The geology of the South Shetland Islands: II. The geology and petrology of Deception Island, Falkland Islands Dependencies Survey Scientific Reports, No. 27, p.43.

Lenn, Y.-D., T. K. Chereskin, and R. C. Glatts. (2003). Seasonal to tidal variability in currents, stratification, and acoustic backscatter in an Antarctic ecosystem at Deception Island. Deep-Sea Res. II, 50, 1665-1684.

Levine, M. D., Padman, L., Muench, R. D., Morison, J. H. (1997). Internal waves and tides in the western Weddell Sea: Observations from Ice Station Weddell. Journal of Geophysical Research, Vol. 102(C1), 1073-1089.

Lopez, O. M., Garcia, A., Gomis, D., Rojas, P., Sospedra, J & Sanchez-Arcilla, A. (1999). Hydrographic and hydrodynamica.characteristics of the eastern basin of the Bransfield Strait (Antartica). Deep-Sea Research I, 46:1755– 1778.

Mão de Ferro, A. (2012), Fontes, transporte e especiação de elementos traço nos compartimentos ambientais da ilha Deception, Antártida. Msc Thesis in Environmental Engineering, Instituto Superior Técnico, Universidade Técnica de Lisboa.

Molina, A., Pablo, M. A. De, & Ramos, M. (2013). 44th Lunar and Planetary Science Conference (2013) 44th Lunar and Planetary Science Conference (2013) (pp. 2–3).

Pereira, A. F., Castro, B. M. (2007). Internal Tides in the Southwestern Atlantic off Brazil: Observations and Numerical Modeling. Journal of physical oceanography, 37, 1512-1517.

Pérez-López, R., Giner-Robles, J. L., Martínez-Díaz, J. J., Rodríguez-Pascua, M. A., Bejar, M., Paredes, C., and González-Casado, J. M. (2007). Active tectonics on Deception Island (West-Antarctica): A new approach by using the fractal anisotropy of lineaments, fault slip measurements and the caldera collapse shape, in Antarctica: A Keystone in a Changing World – Online Proceedings of the 10th ISAES, edited by A.K. Cooper and C.R. Raymond et al., USGS Open-File Report 2007-1047, Short Research Paper 086.

Smith Jr., K.L., Baldwin, R.J., Kaufmann, R.S., Sturz, A. (2003b). Ecosystem studies at Deception Island, Antarctica: an overview. Deep-Sea Research II.

Torrecillas, C. L., Berrocoso, D., Manuel, G. G., Alicia. (2006). The Multidisciplinary Scientific Information Support System (SIMAC) for Deception Island. Vol. XXVIII. Pag. 397-402. En: Antarctica: Contributions to Global Earth Sciences. Berlín, Alemania, Springer.

Trancoso, A. R., Saraiva, S., Fernandes, L., Pina, P., Leitão, P., Neves, R. (2005). Modelling macroalgae using a 3D hydrodynamic-ecological model in a shallow, temperate estuary. Ecological Modelling. 187, 2005, pp. 232–246.

Vaz, N., Dias, J. M., Leitão, P., Martins, I. (2005). Horizontal patterns of water temperature and salinity in an estuarine tidal channel: Ria de Aveiro. Ocean Dynamics. 2005, Vol. 55, pp. 416-429.

Vidal, J., Berrocoso, M., & Fernandez, A. (2010). Study of the tide in Deception and Livingston Islands (Antarctica). Antarctic Science, in press, 2010.